ESC European Society of Cardiology

European Heart Journal (2022) **43**, 2317–2334
https://doi.org/10.1093/eurheartj/ehac109

TRANSLATIONAL RESEARCH
Thrombosis and antithrombotic treatment

Circadian nuclear receptor Rev-erbα is expressed by platelets and potentiates platelet activation and thrombus formation

Jianfeng Shi [1†], Renyang Tong[1†], Meng Zhou [1†], Yu Gao [1], Yichao Zhao[1], Yifan Chen[1], Wenhua Liu[1], Gaoxiang Li[1], Dong Lu[2], Guofeng Meng[2], Liuhua Hu[1], Ancai Yuan [1], Xiyuan Lu[1], and Jun Pu [1]*

[1]Division of Cardiology, State Key Laboratory for Oncogenes and Related Genes, Renji Hospital, School of Medicine, Shanghai Jiao Tong University, Shanghai Cancer Institute, Shanghai, China; and [2]Institute of Interdisciplinary Integrative Medicine Research, Shanghai University of Traditional Medicine, Shanghai, China

Received 29 August 2021; revised 4 February 2022; accepted 22 February 2022; online publish-ahead-of-print 10 March 2022

See the editorial comment for this article 'Chrono-pharmacology-based antiplatelet therapy for acute myocardial infarction', by Simon Tual-Chalot and Konstantinos Stellos, https://doi.org/10.1093/eurheartj/ehac120.

Abstract

Aims Adverse cardiovascular events have day/night patterns with peaks in the morning, potentially related to endogenous circadian clock control of platelet activation. Circadian nuclear receptor Rev-erbα is an essential and negative component of the circadian clock. To date, the expression profile and biological function of Rev-erbα in platelets have never been reported.

Methods and results Here, we report the presence and functions of circadian nuclear receptor Rev-erbα in human and mouse platelets. Both human and mouse platelet Rev-erbα showed a circadian rhythm that positively correlated with platelet aggregation. Global Rev-erbα knockout and platelet-specific Rev-erbα knockout mice exhibited defective in haemostasis as assessed by prolonged tail-bleeding times. Rev-erbα deletion also reduced ferric chloride-induced carotid arterial occlusive thrombosis, prevented collagen/epinephrine-induced pulmonary thromboembolism, and protected against microvascular microthrombi obstruction and infarct expansion in an acute myocardial infarction model. *In vitro* thrombus formation assessed by CD41-labelled platelet fluorescence intensity was significantly reduced in Rev-erbα knockout mouse blood. Platelets from Rev-erbα knockout mice exhibited impaired agonist-induced aggregation responses, integrin αIIbβ3 activation, and α-granule release. Consistently, pharmacological inhibition of Rev-erbα by specific antagonists decreased platelet activation markers in both mouse and human platelets. Mechanistically, mass spectrometry and co-immunoprecipitation analyses revealed that Rev-erbα potentiated platelet activation via oligophrenin-1-mediated RhoA/ERM (ezrin/radixin/moesin) pathway.

Conclusion We provided the first evidence that circadian protein Rev-erbα is functionally expressed in platelets and potentiates platelet activation and thrombus formation. Rev-erbα may serve as a novel therapeutic target for managing thrombosis-based cardiovascular disease.

* Corresponding author. Email: pujun310@hotmail.com
† These authors contributed equally to the study.

Key question

Adverse cardiovascular events have day/night patterns with peaks in the morning, potentially related to endogenous circadian clock control of platelet activation. Whether circadian nuclear receptor Rev-erba is present in platelets and regulates platelet function remains unknown.

Key finding

We provide the first evidence that Rev-erba is functionally expressed in platelets and acts as a positive regulator of platelet activation/thrombus formation through the oligophrenin-1-mediated RhoA/ERM signalling pathway.

Take home message

Our observations highlight the importance of circadian clock machinery in platelet physiology and support the notion that Rev-erba may serve as a novel therapeutic target for managing thrombosis-based cardiovascular diseases.

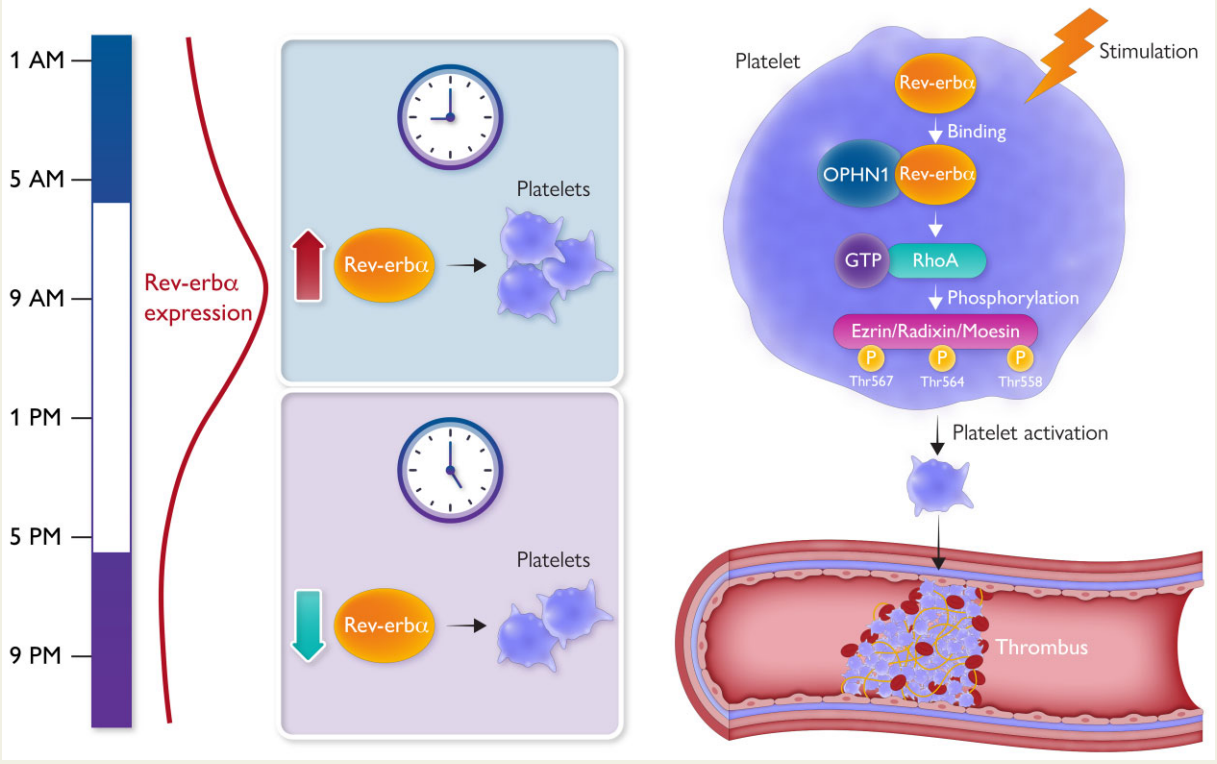

Structured Graphical Abstract Circadian nuclear receptor Rev-erbα potentiates platelet activation and thrombus formation via OPHN-1/RhoA/ERM pathway.

Keywords Circadian • Rev-erbα • Blood platelets • Platelet activation • Thrombosis

Translational Perspective

Adverse cardio-cerebrovascular thrombotic events have day/night patterns with peaks in the morning, potentially related to endogenous circadian clock control of platelet activation. Our study identified circadian nuclear receptor Rev-erbα as a new functional protein being expressed in both human and mouse platelets and exhibiting a circadian rhythm that positively correlated with platelet aggregation. Rev-erbα was significantly upregulated in platelets from acute myocardial infarction patients, with a peak at early morning. Pharmacological inhibition or genetic ablation of Rev-erbα decreases platelet activation and thrombus formation in various thrombosis models. Consistent results of anti-platelet actions were obtained by Rev-erbα-specific antagonists in human platelets. Thus, Rev-erbα may serve as a novel therapeutic target for managing thrombosis-based cardiovascular diseases.

Introduction

Platelets, which are derived from megakaryocytes, are anucleate blood cells that physiologically contribute to haemostasis at sites of vascular injury.[1] However, the pathological activation of platelets triggers occlusive thrombosis and results in ischaemic events, such as myocardial infarction and stroke, which are the leading causes of death globally. Such adverse cardiovascular events follow the

day/night pattern with a peak in the early morning, potentially related to endogenous circadian clock control of platelet activation.[2,3] Multiple measures of platelet activation show strong time-of-day variation, including platelet aggregation and platelet activation markers [i.e. β-thromboglobulin (βTG), platelet factor 4 (PF4), glycoprotein Ib (GPIb), P-selectin, and activated αIIbβ3], which also peak in the early morning at ∼9 a.m.[4–6]

The circadian clock is a ubiquitous endogenous timing system sustaining circadian oscillation that coordinates physiological processes. Circadian nuclear receptor Rev-erbα (also known as nuclear receptor subfamily 1 group D member 1; NR1D1) is a unique member of the nuclear receptor superfamily that was originally cloned in pituitary tissue recognized as a key clock component that provided a feedback loop to consolidate the rhythms of circadian oscillators.[7] Recently, several new functions of Rev-erbα beyond its roles in circadian rhythm were identified, and implied in the pathogenesis of various disorders, such as neoplastic diseases,[8] inflammatory diseases,[9] and cardiometabolic diseases.[10,11] To date, the expression profile and biological function of circadian nuclear receptor Rev-erbα in platelets have never been reported.

In this study, we aim to investigate whether Rev-erbα is expressed by platelets and regulates platelet function. We report our findings that platelet-expressed Rev-erbα displays a circadian rhythm that positively correlates with platelet aggregation. Moreover, Rev-erbα acts as a positive regulator of platelet activation and thrombus formation by regulating oligophrenin-1 (OPHN-1)-mediated RhoA/ERM (ezrin/radixin/moesin) signalling pathway.

Methods

Human studies

All human samples used in this study were processed under Institutional Review Board–approved protocols at Shanghai Jiao Tong University. All study participants were recruited after providing informed consent and with approval by the Ethics Committee of Renji Hospital, School of Medicine, Shanghai Jiao Tong University, and the study was conducted according to the criteria set by the Declaration of Helsinki (2013).

To test the presence of Rev-erbα in human platelets, positive controls including human brain, kidney, and liver samples were obtained from fresh surgical specimens removed for brain, kidney, and liver neoplasia. Normal tissues were collected at least 2 cm away from tumour tissues and were residual tissues that would otherwise have been discarded. Tissues were immediately frozen and stored at −80°C until they were used for analysis. Informed consent was obtained from all the patients before tissue harvest.

To examine the diurnal oscillation of Rev-erbα expression in human platelets, we performed two sets of studies. The first series of studies was conducted among six male and six female healthy volunteers. To avoid potential interference from other confounding factors, we only included volunteers who: (i) aged 20–35 years; (ii) were non-smokers and teetotallers; (iii) had not taken antiplatelet/anticoagulant drugs or other medications in the previous 2 weeks; and (iv) had normal sleep/wake rhythm and none of them had travelled between time zones 3 months before the study.[12] On the day before the study, subjects were admitted to the Cardiovascular Clinical Research Center of Renji Hospital. Blood samples were drawn without stasis from an antecubital vein via indwelling needles. Washed human platelets and platelet-rich plasma (PRP) were prepared as described in the Supplementary material online.

The second series of studies was conducted in 12 male and 8 female patients with acute ST-elevation myocardial infarction (STEMI). ST-elevation myocardial infarction was defined as a clinical syndrome of myocardial ischaemia in association with persistent ECG ST-segment elevations (≥2 mm in two contiguous precordial leads or ≥1 mm in two peripheral leads).[13] To avoid possible interference by other confounding factors, we included patients with first episodes of acute anterior myocardial infarction and in the age range of 50–65 years, and excluded patients if they had: (i) known hypertension, heart failure, structural heart disease, acute pericardial disease, aorta dissection, and diabetes mellitus; and (ii) any history of severe renal or hepatic dysfunction, haematological disorders, infectious disease, autoimmune disease, neurological disease, and cancer. During the same period, healthy donors matched with age and sex were recruited as controls under a separate Institutional Review Board protocol.

Animal studies

All animal experiments were conducted in compliance with the National Institutes of Health Guidelines on the Care and Use of Laboratory Animals (NIH Publication, 8th Edition, 2011), with approval by the Animal Ethics Committee of Shanghai Jiao Tong University. All mice were housed at 24 ± 2°C and 40 ± 5% humidity under a 12-h light/dark cycle with access to diet and water ad libitum. Both male and female mice, aged 8–12-week-old, were used in this study.

C57BL/6J wild type (WT) mice were from Jackson Laboratory. Global Rev-erbα knockout (Rev-erbα$^{-/-}$) mice on a C57BL/6J background were kindly provided by Dr Ueli Schibler (University of Geneva, Geneva, Switzerland).[14] The littermate Rev-erbα$^{+/+}$ mice were used as controls. To generate platelet-specific Rev-erbα knockout (Rev-erbα$^{fl/fl}$PF4Cre^{+}) mice, Rev-erbα$^{fl/fl}$ mice were crossed with the mice carrying the PF4Cre transgene (Jackson Laboratory). The littermate Rev-erbα$^{fl/fl}$PF4Cre^{-} mice were used as controls. The blood samples were collected from the abdominal aorta as described in the Supplementary material online.

Statistical analysis

Data are presented as mean ± standard deviation. Data normality were determined by the Shapiro–Wilk test. When comparing two sets of data, Student's *t*-test (parametric data) or Mann–Whitney U-test (non-parametric data) were used. Multiple group comparisons were performed by a one-way analysis of variance (ANOVA) or two-way ANOVA followed by Tukey's, Dunnett's, or Bonferroni's multiple comparisons. A *P*-value of <0.05 was considered statistically significant. Statistical analysis was performed by the GraphPad Prism 8 software.

Detailed materials and methods are presented in the Supplementary material online.

Results

Rev-erbα is present in human platelets

To our knowledge, the presence of circadian nuclear receptor Rev-erb (including two isoforms: Rev-erbα and Rev-erbβ) in platelets has never been reported. To test the presence of Rev-erbα in platelets, we performed quantitative real-time PCR (qRT-PCR) and western blotting on total mRNA and protein, obtained from human platelets. The human brain, kidney, and liver samples served as positive controls.[15] As shown in *Figure 1A*, Rev-erbα mRNA was detected in human platelets. Immunoblotting confirmed the presence of a Rev-erbα protein band at ∼78 kDa in positive controls (human brain, kidney, and liver samples), as well as in human platelets

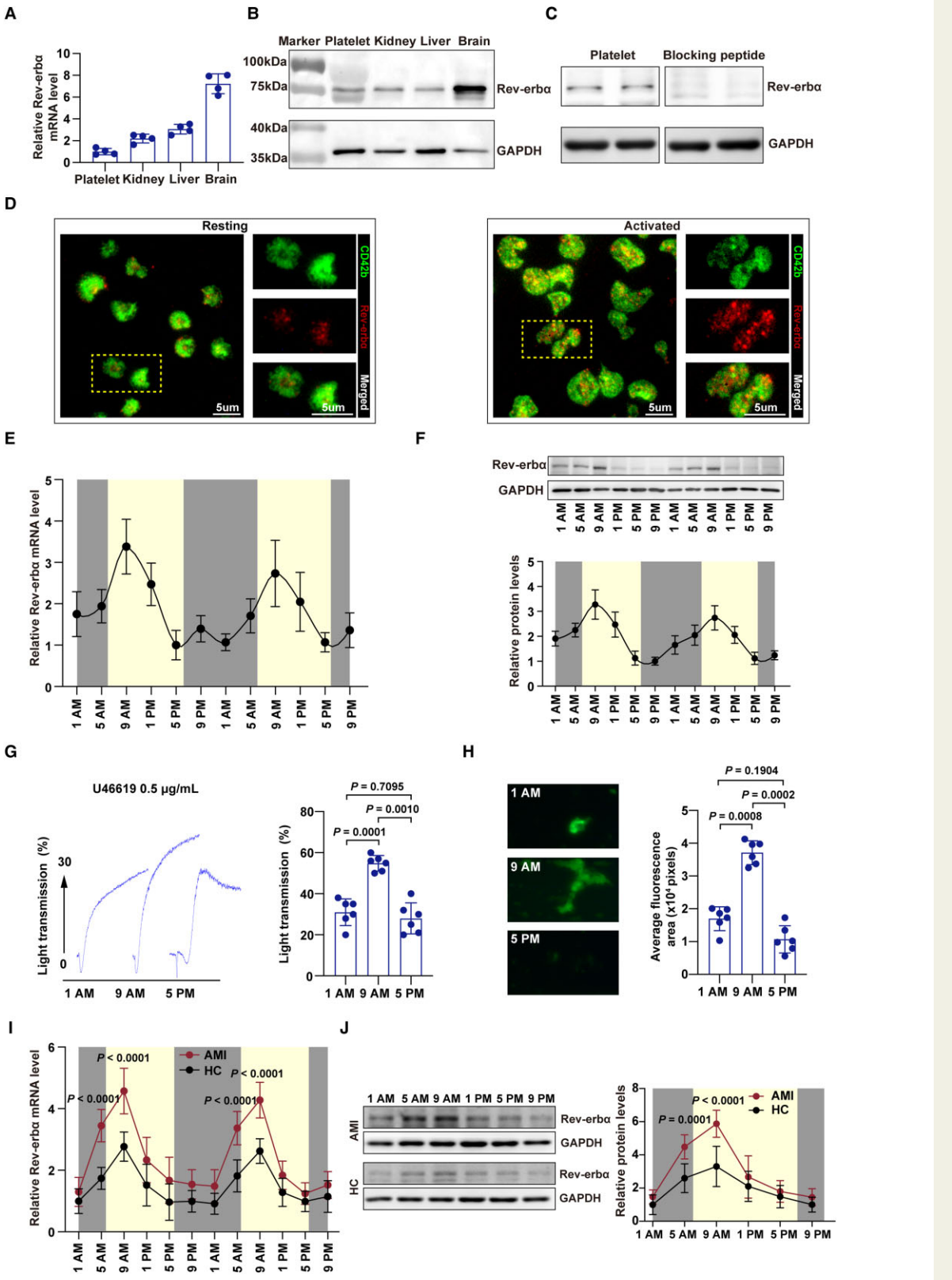

Figure 1 Expression of Rev-erbα in human platelets. (*A*) Lysates of human platelets, kidney, liver, and brain tissues were subjected to quantitative real-time PCR to detect Rev-erbα mRNA ($n = 4$ independent experiments). Kidney, liver, and brain tissues served as positive controls. Glyceraldehyde-3-phosphate dehydrogenase (GAPDH) was used as an internal control. (*B*) Lysates of human platelet, kidney, liver, and brain were subjected to immunoblotting to detect Rev-erbα ($n = 4$ independent experiments). Kidney, liver, and brain tissues served as positive controls. GAPDH was used as an internal control. (*C*) Validation of the Rev-erbα antibody using Rev-erbα blocking peptide to block the antibody

Continued

(*Figure 1B*). This 78 kDa band disappeared on preincubation of the antibody with its immunogenic peptide in human platelets, indicating the specificity of the reaction (*Figure 1C*). The localization of Rev-erbα in human platelets was further analysed by *in situ* immunofluorescence microscopy. In resting platelets, Rev-erbα was found to be dispersed throughout the platelet cytoplasm in a punctate arrangement. While in response to physiological platelet agonists (i.e. U46619, a thromboxane A2 receptor agonist), the localization of Rev-erbα appeared to partially translocate towards the plasma membrane (*Figure 1D*). We did not observe gender differences in the expression of Rev-erbα in human platelets (Supplementary material online, *Figure S1A*). Additionally, we detected the presence of the Rev-erbβ subtype in human platelets (Supplementary material online, *Figure S2A and B*).

The diurnal oscillation of platelet Rev-erbα is associated with the circadian variation in platelet aggregation

Because Rev-erbα protein is an integral component of the circadian rhythm system,[16] we further examined the diurnal oscillation of platelet Rev-erbα expression throughout the day. Importantly, human platelet Rev-erbα expression followed a circadian rhythm-dependent pattern, with a peak corresponding to clock time 9 a.m. (*Figure 1E* and *F*). To investigate whether the diurnal oscillation of platelet Rev-erbα expression is implicated in the circadian rhythm of platelet activation, agonist-induced platelet aggregation responses were examined. A similar circadian variation in platelet activation (agonist-induced aggregation responses, *Figure 1G*) and thrombus propensity (*in vitro* thrombus formation assay, *Figure 1H*) was observed in human platelets, with a peak at 9 a.m. In contrast to that of Rev-erbα, Rev-erbβ expression did not show obvious circadian rhythm-dependent patterns in human platelets (Supplementary material online, *Figure S2C*). Thus, although both Rev-erbα and Rev-erbβ subtypes are present in human platelets, only Rev-erbα expression displays circadian variation.

Adverse cardiovascular events (i.e. acute myocardial infarction) have day/night patterns with peaks in the morning, potentially related to endogenous circadian clock control of platelet activation.[6,17] Thus, we further determined the expression of Rev-erbα in patients with acute STEMI. As shown in *Figure 1I* and *J*, Rev-erbα was significantly upregulated in platelets from acute STEMI patients, with the peak at early morning. No gender differences were observed in the diurnal oscillation pattern of Rev-erbα expression in human platelets (Supplementary material online, *Figure S1B and C*). Together, these data indicate that human platelet Rev-erbα shows a circadian rhythm that positively correlates with platelet aggregation.

Rev-erbα is present in mouse platelets

We further determined the expression profile of circadian nuclear receptor Rev-erbα in mouse platelets. As shown in *Figure 2A* and *B*, Rev-erbα mRNA and protein were detected in mouse platelets. The Rev-erbα protein appeared at an expected molecular weight of ~78 kDa in platelets obtained from mice, but was not detected in platelets obtained from Rev-erbα-deficient mice (*Figure 2C*). *In situ* immunofluorescence confirmed the presence of Rev-erbα in mouse platelets. Similar to the human platelets, Rev-erbα was found to be dispersed throughout the platelet cytoplasm in a punctate arrangement in resting mouse platelets, and appeared to partially translocate towards the plasma membrane upon stimulation by agonists (*Figure 2D*).

Next, we examined the diurnal oscillation of Rev-erb expression in mouse platelets throughout the day by qRT-PCR and western blotting (Supplementary material online, *Figure S3A* and *Figure 2E*). For mice, we used zeitgeber time (ZT), which is a standardized 24-h notation of the phase in an entrained circadian cycle.[18] The Rev-erbα expression followed a circadian rhythm-dependent pattern in mouse platelets, with a peak at ZT4 and a trough at ZT16. We did not observe gender differences in Rev-erbα expression and circadian variation in mouse platelets (Supplementary material online, *Figure S1D and E*). Platelets are anucleate cells derived from megakaryocytes.[19] Thus, we examined Rev-erbα expression in mouse megakaryocytes. We did not observe gender differences in Rev-erbα expression in

Figure 1 Continued

epitope ($n = 3$ independent experiments). (*D*) Immunolocalization of Rev-erbα in human platelets. Resting and activated platelets were fixed in 4% paraformaldehyde-PBS. Platelets were permeabilized and stained with anti-CD42b (GPIbα) and anti-Rev-erbα antibodies. Activated platelets were prepared by treatment with U46619 (0.5 μg/ml) in the presence of Integrilin (4 μM). (*E*) Platelet levels of Rev-erbα mRNA determined by quantitative real-time PCR ($n = 6$ per time point). Variation was analysed by one-way repeated measures analysis of variance ($P = 0.0001$). (*F*) Platelet levels of Rev-erbα protein determined by western blotting ($n = 6$ per time point). Data were analysed by one-way repeated measures ANOVA test. Variation was analysed by one-way repeated measures analysis of variance ($P < 0.0001$). (*G*) Platelets collected at 1 a.m., 9 a.m., and 5 a.m. were used for aggregation tests. U46619 (0.5 μg/ml) was used as inducing agents. The maximum aggregation was compared ($n = 6$ per time point). Data were analysed by one-way repeated measures ANOVA test followed by Tukey's multiple comparisons test. (*H*) Representative images of microfluidic chambers through which D-phenylalanyl-L-prolyl-L-arginine chloromethyl ketone-anticoagulated blood from 1 a.m., 9 a.m. and 5 p.m., labelled with CD41 was passed on immobilized collagen at a shear rate of 20 dyn for 3 min. Representative images were captured at ×4 magnification under an EVOS microscope, and the average fluorescence area was compared ($n = 6$ per time point). Data were analysed by one-way repeated measures ANOVA test followed by Tukey's multiple comparisons test. (*I*) Platelet levels of Rev-erbα mRNA in acute ST-elevation myocardial infarction patients and healthy controls determined by quantitative real-time PCR ($n = 12$ per time point). Data were analysed by two-way repeated measures ANOVA test followed by Bonferroni *post hoc* analysis. (*J*) Platelet levels of Rev-erbα protein in acute ST-elevation myocardial infarction patients and healthy control were determined by western blotting, and the band intensity was quantified ($n = 12$ per time point). Data were analysed by two-way repeated measures ANOVA test followed by Bonferroni *post hoc* analysis. AMI indicates acute myocardial infarction; HC, healthy controls.

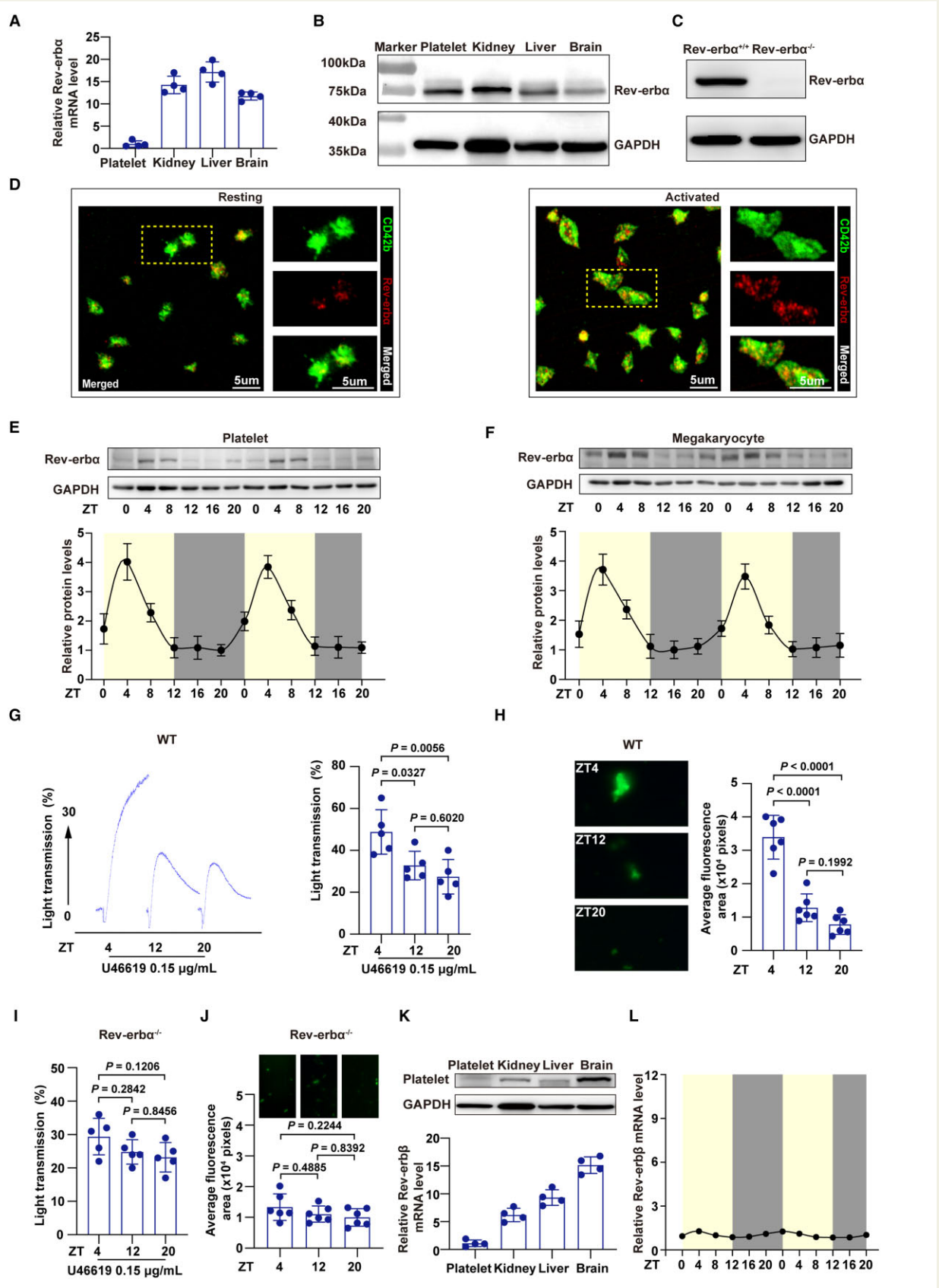

Figure 2 Expression of Rev-erbα in the mouse platelets. (*A*) Lysates of C57BL/6J wild type mouse platelets, kidney, liver, and brain tissues were subjected to quantitative real-time PCR to detect Rev-erbα mRNA ($n = 4$ independent experiments). Kidney, liver, and brain tissues served as

Continued

mouse megakaryocytes (Supplementary material online, *Figure S1F*). We further examined the diurnal oscillation of Rev-erbα expression in mouse megakaryocytes throughout the day (Supplementary material online, *Figure S3B* and *Figure 2F*). Similarly, Rev-erbα expression demonstrated a diurnal oscillation in mouse megakaryocytes. Moreover, a day/night fluctuation in the platelet aggregation rates and *in vitro* thrombus propensity was also observed in mice, with a peak at ZT4 (*Figure 2G* and *H*). Deletion of Rev-erbα impaired the diurnal oscillation of platelet aggregation and thrombus propensity (*Figure 2I* and *J*). Although we also detected the presence of Rev-erbβ subtype in mouse platelets (*Figure 2K*), its expression did not show obvious circadian rhythm-dependent patterns in mouse platelets (*Figure 2L*). Together, our data confirm that Rev-erbα is present in mouse platelets, and displays a circadian rhythm that positively correlates with platelet aggregation.

Rev-erbα deletion in mice prolongs bleeding time

To determine whether Rev-erbα is involved in regulating platelet function, global Rev-erbα knockout mice (Rev-erbα$^{-/-}$) were first used. Rev-erbα$^{-/-}$ mice were fertile and healthy without visible abnormalities, spontaneous bleeding or thrombosis. Compared with Rev-erbα$^{+/+}$ mice, Rev-erbα$^{-/-}$ mice exhibited significantly prolonged tail-bleeding time, and larger ratios of bleeding time ≥15 min (Supplementary material online, *Figure S4A and B*). However, Rev-erbα$^{-/-}$ mice and Rev-erbα$^{+/+}$ littermates did not differ in platelet counts, average platelet sizes, white blood cell counts, red blood cell counts, haemoglobin, activated partial thromboplastin time (APTT), prothrombin time (PT), or international normalized ratio (INR) (Supplementary material online, *Figure S4C–J*). To further confirm the role of platelet-expressed Rev-erbα, we generated conditional Rev-erbα knockout mice (Rev-erbα$^{fl/fl}$PF4Cre^{+}), in which Cre-recombinase was under the control of the platelet factor 4 (PF4) promoter, recombining almost exclusively in platelets and megakaryocytes (*Figure 3A*). The platelet-specific deletion of Rev-erbα was confirmed at DNA, mRNA, and protein levels (*Figure 3B* and *C*). No statistical differences were detected in the expression of other circadian proteins between Rev-erbα$^{fl/fl}$PF4Cre^{-} and Rev-erbα$^{fl/fl}$PF4Cre^{+} platelets (Supplementary material online, *Figure S5*).

Consistently, Rev-erbα$^{fl/fl}$PF4Cre^{+} mice exhibited a prolonged bleeding time (*Figure 3D*) and larger ratios of bleeding time ≥15 min following tail transection when compared with Rev-erbα$^{fl/fl}$PF4Cre^{-} mice (*Figure 3E*). Rev-erbα$^{fl/fl}$PF4Cre^{+} and Rev-erbα$^{fl/fl}$PF4Cre^{-} mice did not differ in platelet counts (*Figure 3F*), average platelet sizes (*Figure 3G*), the platelet microstructures (α-granules and dense granules) (*Figure 3H* and *I*) or the expression levels of the major platelet membrane proteins, CD41, and GPVI (*Figures 3J*). These results suggest that Rev-erbα deletion impairs haemostasis without altering platelet counts and microstructures.

Rev-erbα deletion in mice decreases thrombus propensity

We used different thrombosis models to determine the effects of Rev-erbα deficiency on thrombus propensity. In the first model,

Figure 2 Continued

positive controls. GAPDH was used as an internal control. (*B*) Lysates of wild type mouse platelets, kidney, liver, and brain tissues were subjected to immunoblotting to detect Rev-erbα protein ($n = 4$ independent experiments). Kidney, liver, and brain tissues served as positive controls. GAPDH was used as a loading control. (*C*) Rev-erbα protein expression by immunoblotting in platelets from Rev-erbα$^{+/+}$ and Rev-erbα$^{-/-}$ mice. The Rev-erbα protein appeared in platelets obtained from Rev-erbα$^{+/+}$ mice, but was not detected in platelets obtained from Rev-erbα$^{-/-}$ mice ($n = 3$ independent experiments). (*D*) Immunolocalization of Rev-erbα in wild type mouse platelets was analysed using immunofluorescence microscopy. Resting and activated [using U46619 (0.15 μg/ml) in the presence of Integrilin (4 μM)] platelets were fixed in 4% (v/v) paraformaldehyde-PBS. Platelets were permeabilized and stained with anti-CD41 (αIIbβ3) and anti-Rev-erbα antibodies. (*E*) Wild type mouse platelet levels of Rev-erbα protein determined by western blotting ($n = 4$ per time point) every 4 for 48 h. Variation was analysed by one-way ANOVA ($P < 0.0001$). (*F*) Wild type mouse megakaryocyte levels of Rev-erbα protein determined by western blotting ($n = 4$ per time point) every 4 for 48 h. Variation was analysed by one-way ANOVA ($P < 0.0001$). (*G*) Wild type mouse platelets collected at ZT4, ZT12, and ZT20 were used for aggregation. U46619 (0.15 μg/ml) was used as an inducing agent. The maximum aggregation was compared ($n = 5$ independent experiments). Data were analysed by one-way ANOVA test followed by Tukey's multiple comparisons test. (*H*) Representative images of microfluidic chambers through which D-phenylalanyl-L-prolyl-L-arginine chloromethyl ketone (PPACK)-anticoagulated wild type mouse whole blood from ZT4, ZT12, and ZT20, labelled with CD41 was passed on immobilized collagen for 3 min. Representative images were captured at ×4 magnification under an EVOS microscope, and the average fluorescence area was compared ($n = 6$ per time point). Data were analysed by one-way ANOVA test followed by Tukey's multiple comparisons test. The average fluorescence area was compared across groups. (*I*) Rev-erbα$^{-/-}$ mouse platelets collected at ZT4, ZT12, and ZT20 were used for aggregation. U46619 (0.15 μg/ml) was used as an inducing agent. The maximum aggregation was compared ($n = 5$ independent experiments). Data were analysed by one-way ANOVA test followed by Tukey's multiple comparisons test. (*J*) Representative images of microfluidic chambers through which D-phenylalanyl-L-prolyl-L-arginine chloromethyl ketone(PPACK)-anticoagulated Rev-erbα$^{-/-}$ mouse whole blood from ZT4, ZT12, and ZT20, labelled with CD41 was passed on immobilized collagen for 3 min. Representative images were captured at ×4 magnification under an EVOS microscope, and the average fluorescence area was compared ($n = 6$ per time point). Data were analysed by one-way ANOVA test followed by Tukey's multiple comparisons test. The average fluorescence area was compared across groups. (*K*) Lysates of wild type mouse platelets, kidney, liver, and brain were subjected to immunoblotting to detect Rev-erbβ. Kidney, liver, and brain tissues served as positive controls. GAPDH was used as a loading control. Lysates of wild type mouse platelets, kidney, liver, and brain tissues were subjected to qRT-PCR to detect Rev-erbβ mRNA. Kidney, liver, and brain tissues served as positive controls. GAPDH was used as an internal control. (*L*) Wild type mouse Rev-erbβ mRNA level was determined every 4 for 48 h ($n = 4$ per time point). Variation was analysed by one-way ANOVA ($P > 0.05$).

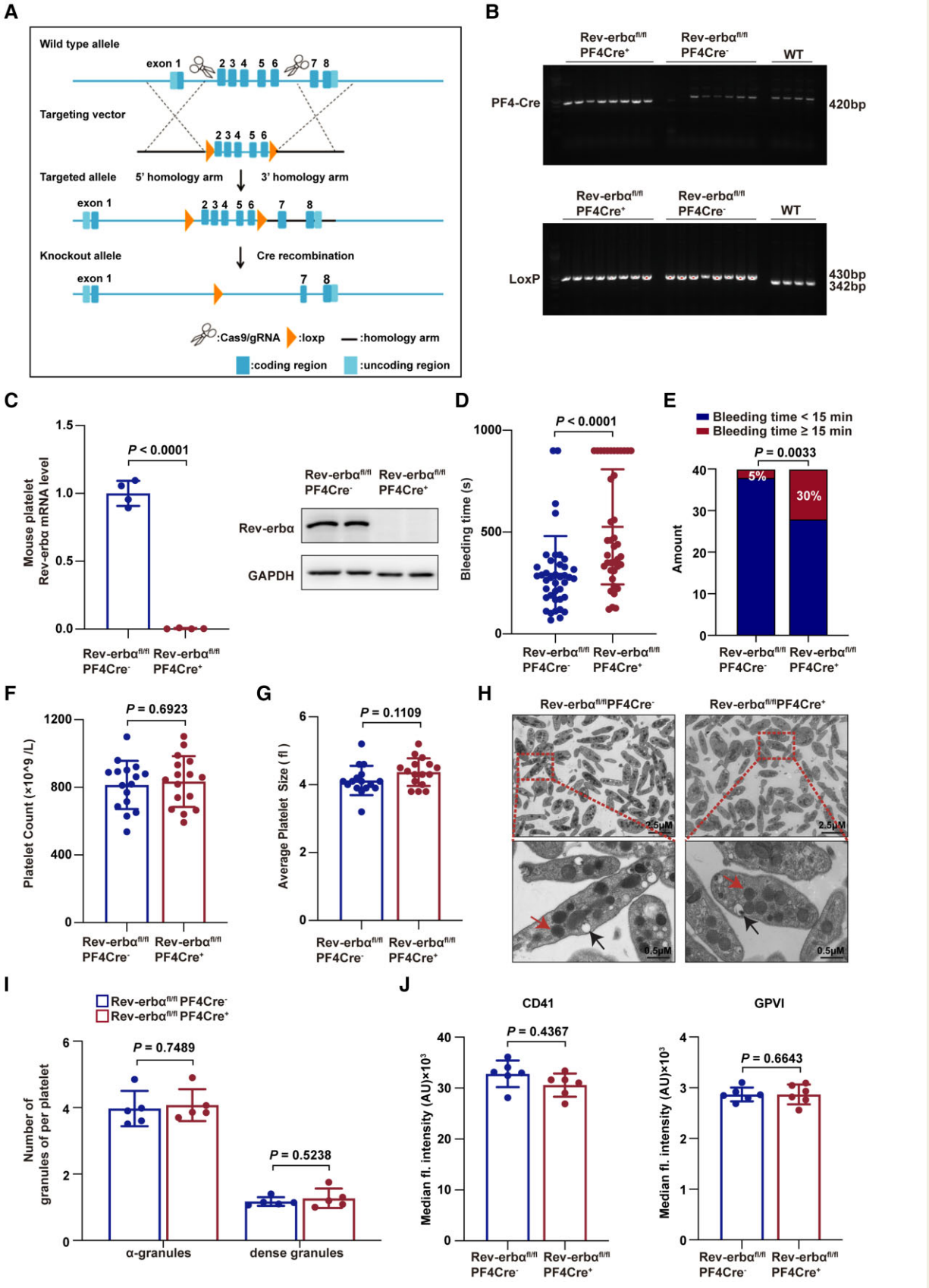

Figure 3 Platelet-specific deletion of Rev-erbα impaired haemostasis. (*A*) Schematic of Rev-erbα gene editing strategy. To generate platelet-specific Rev-erbα knockout (Rev-erbα$^{fl/fl}$PF4Cre^{+}) mice, Rev-erbα$^{fl/fl}$ mice were crossed with the mice carrying the PF4Cre transgene. The

Continued

the time to occlusion in the $FeCl_3$-induced carotid artery thrombosis assay was analysed using the laser speckle imaging technique.[20] The mean time to occlusion in Rev-erbα$^{fl/fl}$PF4Cre^{+} mice was significantly longer than that in Rev-erbα$^{fl/fl}$PF4Cre^{-} mice (11.30 $\pm$ 2.96 min vs. 6.86 $\pm$ 0.71 min; $P < 0.05$) (*Figure 4A*). The thrombus cross-sectional area of the $FeCl_3$-injured carotid artery segment in Rev-erbα$^{fl/fl}$PF4Cre^{+} mice was significantly smaller than that in Rev-erbα$^{fl/fl}$PF4Cre^{-} mice (*Figure 4B*). In the second model, a collagen/epinephrine-induced thromboembolism assay was performed in the absence of endothelial influence. The inability of Evan's blue dye to penetrate the lungs because of obstruction (i.e. pink colour) was severer in Rev-erbα$^{fl/fl}$PF4Cre^{-} mice than that in Rev-erbα$^{fl/fl}$PF4Cre^{+} mice (*Figure 4C*). Moreover, the number of pulmonary vasculature thrombi in the pulmonary sections of Rev-erbα$^{fl/fl}$PF4Cre^{+} mice was less than that in the pulmonary sections of Rev-erbα$^{fl/fl}$PF4Cre^{-} mice (*Figure 4D*). To further evaluate the thrombus growth in the absence of the influence of the endothelium, we assayed *in vitro* thrombus formation by perfusing whole blood through a microfluidic device coated with fibrillar collagen.[21] The number of CD41-labelled platelets in a thrombus (a measure of thrombus size determined based on the fluorescence intensity of CD41-labelled platelets) in Rev-erbα$^{fl/fl}$PF4Cre^{+} mouse blood was significantly lower than that in Rev-erbα$^{fl/fl}$PF4Cre^{-} mouse blood (*Figure 4E*). These results indicate that Rev-erbα acts as a positive regulator of thrombus formation. The prothrombotic role of platelet-expressed Rev-erbα was further confirmed using a platelet depletion/reconstitution mouse model (detailed in Supplementary material online, *Figures S6 and S7*).

Microvascular microthrombi obstruction contributes to myocardial infarct expansion and heart dysfunction.[22] Thus, we further evaluated the effects of platelet Rev-erbα deletion in a model of acute myocardial infarction.[22] Acute myocardial infarction was induced by ligation of the left anterior descending coronary artery, and microthrombi obstruction, infarct area, myocardial viability, and cardiac function were evaluated as described previously.[22] Compared with Rev-erbα$^{fl/fl}$PF4Cre^{-} mice, Rev-erbα$^{fl/fl}$PF4Cre^{+} mice exhibited less microthrombi (*Figure 5A*), reduced infarct area, and improved myocardial viability and cardiac dysfunction (*Figure 5B*). Thus, platelet Rev-erbα deletion protects against microvascular microthrombi obstruction and infarct expansion in a model of acute myocardial infarction.

Rev-erbα deletion decreases platelet aggregation and multiple aspects of platelet activation

Platelet aggregation

The prothrombotic mechanisms of Rev-erbα were further studied by analysing platelet function in Rev-erbα$^{fl/fl}$PF4Cre^{-} and Rev-erbα$^{fl/fl}$PF4Cre^{+} mice. The Rev-erbα$^{fl/fl}$PF4Cre^{-} and Rev-erbα$^{fl/fl}$PF4Cre^{+} platelets were stimulated with various physiological agonists. The platelet aggregation responses in washed mouse platelets were analysed using light transmission aggregometry. Compared with that of Rev-erbα$^{fl/fl}$PF4Cre^{-} platelets, the aggregation of Rev-erbα$^{fl/fl}$PF4Cre^{+} platelets significantly decreased upon stimulation with low concentrations of U46619 (0.1 and 0.15 μg/ml) (*Figure 6A*). Similar results were obtained on the aggregation of Rev-erbα$^{fl/fl}$PF4Cre^{+} platelets in response to low concentrations of thrombin, collagen or ADP (shown in Supplementary material online, *Figure S8A–C*). The aggregation defects were overcome by a high dose of agonists. These results suggest that Rev-erbα deletion inhibits platelet aggregation.

Platelet α-granule release

Platelet α-granule release was evaluated by detecting the expression of P-selectin, a glycoprotein, that is, located within the α-granule membrane of non-activated platelets and translocated to the platelet surface in activated platelets.[23] Compared with that of Rev-erbα$^{fl/fl}$PF4Cre^{-} platelets, P-selectin surface expression of Rev-erbα$^{fl/fl}$PF4Cre^{+} platelets was significantly decreased upon stimulation with agonists, as assessed by the flow cytometric analysis (*Figure 6B*).

Fibrinogen-binding and JON/A-binding

Integrin αIIbβ3 is the most abundant glycoprotein on the platelet surface that mediates multiple aspects of platelet signalling.[24] Integrin αIIbβ3 inside-out activation was evaluated by measuring fibrinogen-binding using flow cytometry detection of Alexa Fluor 647-labelled fibrinogen-binding and PE-labelled JON/A-binding to platelets. In response to agonist treatment, fibrinogen-binding and JON/A-binding on Rev-erbα$^{fl/fl}$PF4Cre^{+} platelets were significantly lower than those on Rev-erbα$^{fl/fl}$PF4Cre^{-} platelets (*Figure 6C*).

Figure 3 Continued

littermate Rev-erbα$^{fl/fl}$PF4Cre^{-} mice were used as controls. (*B*) PCR analysis for the confirmation of gene editing. The 420 bp band represents PF4Cre. The 430 bp represents the mutation, which was produced by the insertion of LoxP in intron 1 and intron 6. The 342 bp represents the wild type. (*C*) Platelet levels of Rev-erbα mRNA and protein in indicated groups determined by qRT-PCR ($n = 4$ independent experiments) and western blotting ($n = 4$ independent experiments). Data were analysed by Student's *t*-test. (*D*) Bleeding time for Rev-erbα$^{fl/fl}$PF4Cre^{-} and Rev-erbα$^{fl/fl}$PF4Cre^{+} mice. Each symbol represents a single mouse. Means are indicated by horizontal lines. Data were analysed by Mann–Whitney U-test. Results were obtained from 40 Rev-erbα$^{fl/fl}$PF4Cre^{-} and 40 Rev-erbα$^{fl/fl}$PF4Cre^{+} mice. (*E*) Percentages of Rev-erbα$^{fl/fl}$PF4Cre^{-} and Rev-erbα$^{fl/fl}$PF4Cre^{+} mouse bleeding times ≥15 min or were <15 min. Data were analysed by χ^2-test. Results were obtained from 40 Rev-erbα$^{fl/fl}$PF4Cre^{-} and 40 Rev-erbα$^{fl/fl}$PF4Cre^{+} mice. (*F* and *G*) Platelet counts and platelet average sizes were analysed (16 from Rev-erbα$^{fl/fl}$PF4Cre^{-} mice and 16 from Rev-erbα$^{fl/fl}$PF4Cre^{+} mice). Data were analysed by Student's *t*-test. (*H*) Electron microscopic images of Rev-erbα$^{fl/fl}$PF4Cre^{-} and Rev-erbα$^{fl/fl}$PF4Cre^{+} platelet ultrastructure (red arrows, α-granules; black arrows, dense granules). (*I*) Quantification of α-granules and dense granules of Rev-erbα$^{fl/fl}$PF4Cre^{-} and Rev-erbα$^{fl/fl}$PF4Cre^{+} platelets. Under 3000 magnification, α-granules and dense granules in platelets (50 from Rev-erbα$^{fl/fl}$PF4Cre^{-} and 44 from Rev-erbα$^{fl/fl}$PF4Cre^{+}) were counted. Data were analysed by Student's *t*-test. (*J*) Surface expression of CD41 and GPVI in indicated groups. Data were analysed by Student's *t*-test. GPVI indicates glycoprotein VI; WT indicates wild type.

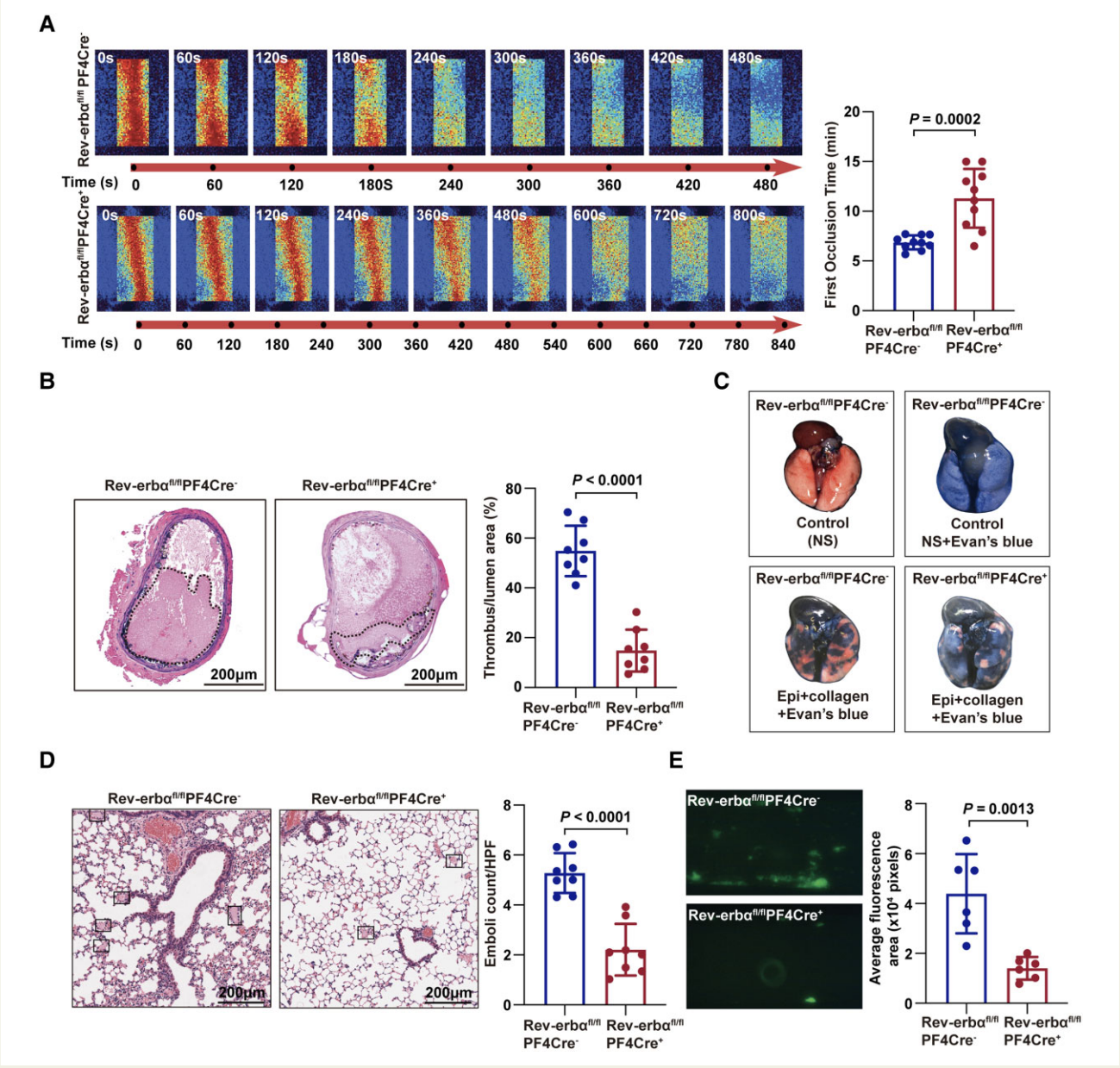

Figure 4 Platelet-specific deletion of Rev-erbα decreased thrombus formation *in vivo* and *in vitro*. (*A*) Representative images of blood flow through carotid vascular which damaged by 10% $FeCl_3$. The blood flow was detected using the laser speckle imaging technique. The red part, which represented the blood flow signal, became weak and finally disappeared as time went on. The mean times of the first occlusion in Rev-erbα$^{fl/fl}$PF4Cre^{-} and Rev-erbα$^{fl/fl}$PF4Cre^{+} mice were shown. Quantification of the first occlusion time in Rev-erbα$^{fl/fl}$PF4Cre^{-} and Rev-erbα$^{fl/fl}$PF4Cre^{+} mice ($n = 10$ per group). Data were analysed by Student's *t*-test. (*B*) The ratio of thrombosis cross-sectional area to lumen cross-sectional area was analysed. Scale bar = 200 μm. Quantification of the ratio of thrombosis area to lumen area in Rev-erbα$^{fl/fl}$PF4Cre^{-} and Rev-erbα$^{fl/fl}$PF4Cre^{+} mice ($n = 8$ per group). Data were analysed by Student's *t*-test. (*C*) Images of the mouse lungs injected with 0.5 ml of Evans blue solution (1% in saline) into the heart 5 min after the injection of the collagen–epinephrine mix. The inability of Evan's blue dye to penetrate the lungs was visible from their pink colour. Mouse lungs were blue due to the free passage of the dye ($n = 8$ per group). (*D*) Images of haematoxylin and eosin-stained paraffin-embedded sections of the lungs from (*C*). Scale bar = 200 μm. Quantification of the number of lung embolisms ($n = 8$ per group). Data were analysed by Student's *t*-test. (*E*) Representative images of microfluidic chambers through which D-phenylalanyl-L-prolyl-L-arginine chloromethyl ketone-anticoagulated blood from Rev-erbα$^{fl/fl}$PF4Cre^{-} and Rev-erbα$^{fl/fl}$PF4Cre^{+} mice labelled with CD41 was passed on immobilized collagen at a shear rate of 20 dyn for 3 min. Representative images were captured at ×4 magnification under an EVOS microscope. The percentage of fluorescence intensity was analysed with Image J (National Institutes of Health). Quantification of the fluorescence intensity ($n = 6$ independent experiments). Data were analysed by Student's *t*-test.

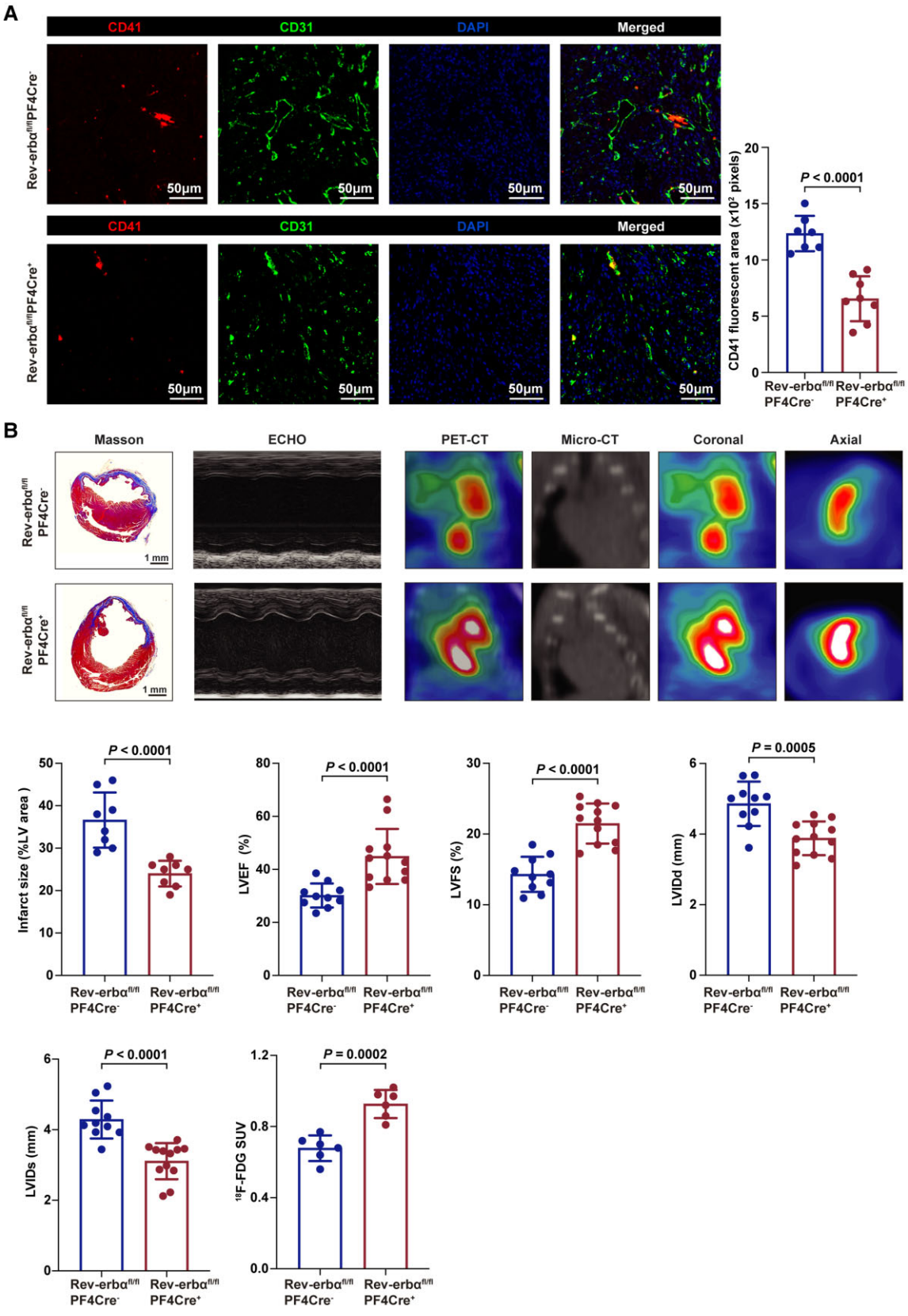

Figure 5 Platelet-specific deletion of Rev-erbα protected against microvascular microthrombi obstruction and infarct expansion. (*A*) Immunofluorescence of the hearts from Rev-erbα$^{fl/fl}$PF4Cre^{-} and Rev-erbα$^{fl/fl}$PF4Cre^{+} post-acute myocardial infarction. Platelets, endothelial cells

Continued

Clot retraction

Clot retraction is an outside-in signalling event downstream of αIIbβ3 integrin activation.[25] Compared with Rev-erbα$^{fl/fl}$PF4Cre^{-} platelets, the Rev-erbα$^{fl/fl}$PF4Cre^{+} platelets exhibited significantly decreased clot retraction in PRP (*Figure 6D*). Collectively, these results suggest that genetic Rev-erbα inhibition impairs platelet aggregation and activation.

Pharmacological inhibition of Rev-erbα decreases platelet aggregation and multiple aspects of platelet activation

We further tested the effects of pharmacological Rev-erbα inhibition in both mouse and human platelets. To date, only two Rev-erbα antagonists, SR8278, and GSK2945, have been described.[26,27] SR8278 was identified as the first Rev-erbα antagonist for probing Rev-erbα function;[26] however, whether GSK2945 is an agonist or antagonist is not conclusive so far.[27,28] Thus, we selected SR8278 as a pharmacological inhibitor in our study, and performed molecular docking research to investigate the binding affinity and the target binding sites between SR8278 and the Rev-erbα receptor. The crystal structure of human Rev-erbα (Homo sapiens, PDB id: 3N00) was downloaded from the RCSB Protein Data Bank (PDB, https://www.rcsb.org/). The mouse Rev-erbα structure (*Mus musculus*) was obtained by homology modelling due to no crystal structure in PDB. The docking scores, which represent the affinity between SR8278 and Rev-erbα proteins, were −6.8520 kcal/mol for humans and −6.5848 kcal/mol for mice (Supplementary material online, *Figure S9A*). According to the two-dimensional interaction map, human Rev-erbα complexed with SR8278, with an arene–arene interaction at Phe128 of human Rev-erbα, and a H-bond at Met166 of human Rev-erbα. Moreover, there existed hydrophobic interactions between SR8278 and human Rev-erbα, which were helpful to make the ligands bind in the pocket more stably (Supplementary material online, *Figure S9B*). Taken together, the molecular docking confirmed the stable interaction between SR8278 and Rev-erbα.

Next, washed platelets were pre-treated with Rev-erbα antagonist SR8278 (10–50 μM) before platelet activation tests. SR8278 concentration dependently inhibited mouse platelet aggregation induced by U46619 (0.15 μg/ml) (*Figure 7A*). Treatment with 30 and 50 μM SR8278 significantly inhibited the U46619-induced α-granule release, as evidenced by reduced P-selectin expression in mouse platelets (*Figure 7B*). Moreover, treatment with 10, 30, or 50 μM SR8278 inhibited integrin αIIbβ3 inside-out activation (i.e. fibrinogen-binding and JON/A-binding) induced by U46619 in mouse platelets (*Figure 7C*). Furthermore, SR8278 concentration dependently decreased the average ratio of clot retraction of PRP (*Figure 7D*).

To corroborate the role of Rev-erbα in human platelet aggregation and activation, SR8278-pre-treated human platelets were subjected to various platelet activation tests. SR8278 concentration dependently inhibited agonist-induced aggregation responses (*Figure 7E*), P-selectin expression (*Figure 7F*), fibrinogen-binding, PAC-1 binding (*Figure 7G*), and clot retraction (*Figure 7H*). Note that the effective concentrations of Rev-erbα-specific antagonist SR8278 on human platelet aggregation/activation were higher than those on mouse platelet aggregation/activation. Together, these results suggest that pharmacological inhibition of Rev-erbα significantly inhibits human and mouse platelet aggregation and activation.

Rev-erbα regulates OPHN-1-mediated RhoA/ERM signalling in platelets

To further elucidate the potential molecular mechanisms of the role of Rev-erbα in platelet activation, the Rev-erbα-interacting proteins were characterized using immunoprecipitation and mass spectrometry. Based on the results of mass spectrometry and the protein–protein interaction network analysis using String and UniProt, OPHN-1 was identified as a potential candidate for further analysis (*Figure 8A*). Oligophrenin-1 is a GTPase-activating protein (GAP) in platelets that exhibits strong GTPase-stimulating activity towards the Rho-family small GTPases RhoA, which was crucial for platelet activation.[29] The results of the co-immunoprecipitation revealed that Rev-erbα coimmunoprecipitated with OPHN-1 in both mouse and human platelets and this interaction significantly increased upon stimulation with agonist U46619 (*Figure 8B*). To further identify the role of Rev-erbα in OPHN-1 mediated signalling, the activity of RhoA, a main downstream target of OPHN-1, was analysed. Rev-erbα deletion significantly downregulated the activity of RhoA (*Figure 8C*) without altering RhoA expression in mouse platelets (*Figure 8D*). Besides, the phosphorylation levels of ERM (ezrin/radixin/moesin) proteins, a downstream effector of RhoA, were significantly downregulated in Rev-erbα$^{fl/fl}$PF4Cre^{+} platelets stimulated with U46619 at the corresponding time points (*Figure 8E*). Similar results were obtained in the pharmacological inhibition experiments with Rev-erbα-specific antagonists in human platelets. Pre-treatment by SR8278 inhibited the activity of RhoA (*Figure 8F*) without affecting RhoA expression (*Figure 8G*), and reduced the phosphorylation levels of ERM (*Figure 8H*) in human platelets in a concentration-dependent manner. However, SR8278 lost its inhibition ability on platelet aggregation, RhoA activation, and ERM phosphorylation in OPHN-1$^{-/+}$ platelets (Supplementary material online, *Figure S10*). Taken together, these results suggest that Rev-erbα

Figure 5 Continued

and nuclei were stained with anti-CD41, anti-CD31, and 4',6-diamidino-2-phenylindole. Scale bars = 50 μm. Quantification of CD41 area per field ($n = 7$–8 per group). Data were analysed by Student's *t*-test. (*B*) Representative images of Masson's trichrome-stained hearts, M-mode echocardiography, and positron emission tomography computed tomography scanning of Rev-erbα$^{fl/fl}$PF4Cre^{-} and Rev-erbα$^{fl/fl}$PF4Cre^{+} mice on day seven post-acute myocardial infarction. Quantification of infarct size ($n = 8$ per group), echocardiographic cardiac function ($n = 10$–12 per group), and mean myocardial ^{18}F-FDG SUV ($n = 6$ per group). Data were analysed by Student's *t*-test. ECHO indicates echocardiography; ^{18}F-FDG SUV, 18F-fluorodeoxyglucose standardized uptake value; LV, left ventricular; LVEF, left ventricular ejection fraction; LVFS, left ventricularfractional shortening; LVIDs, left ventricularinternal dimension in systole; LVIDd, left ventricular internal dimension in diastole; PET-CT, positron emission tomography computed tomography.

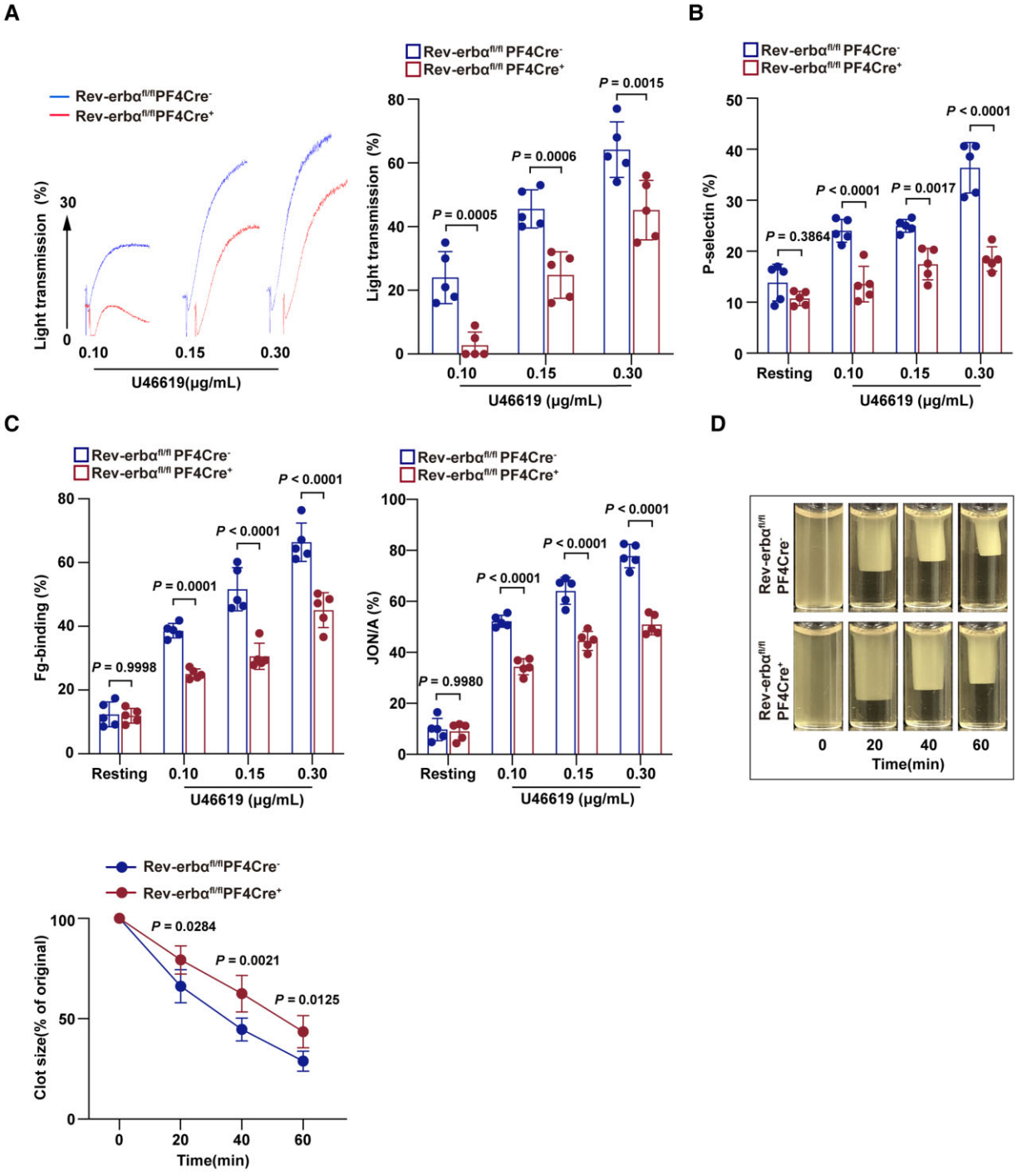

Figure 6 Platelet-specific deletion of Rev-erbα decreased multiple aspects of platelet activation. (*A*) Representative platelet aggregation tracings of washed platelets from Rev-erbα$^{fl/fl}$PF4Cre^{-} or Rev-erbα$^{fl/fl}$PF4Cre^{+} mouse stimulated with various concentrations of U46619, as indicated. Aggregation was measured as a change in light transmission and monitored for 5 min. Data are plotted in terms of percentage aggregation ($n =$ 5 independent experiments). Data were analysed by one-way ANOVA followed by Bonferroni *post hoc* analysis. (*B*) Quantitation of P-selectin surface expression of Rev-erbα$^{fl/fl}$PF4Cre^{-} or Rev-erbα$^{fl/fl}$PF4Cre^{+} mouse platelets stimulated with various concentrations of U46619, as indicated ($n = 5$ independent experiments). Data were analysed by two-way ANOVA test followed by Bonferroni *post hoc* analysis. (*C*) Quantitation of flow cytometric analysis of Alexa Fluor 647-labelled fibrinogen-binding and PE-labelled JON/A-binding to Rev-erbα$^{fl/fl}$PF4Cre^{-} or Rev-erbα$^{fl/fl}$PF4Cre^{+} mouse platelets stimulated with various concentrations of U46619, as indicated. Data are presented as a percentage of platelets binding to fibrinogen ($n = 5$ independent experiments). Data were analysed by two-way ANOVA test followed by Bonferroni *post hoc* analysis. (*D*) The representative images of Rev-erbα$^{fl/fl}$PF4Cre^{-} and Rev-erbα$^{fl/fl}$PF4Cre^{+} mouse platelet clot retraction stimulated with 0.5 U/ml thrombin. Images were captured every 20 for 60 min. The two-dimensional size of the clot was measured using the ImageJ software. The data are presented in terms of clot size ($n = 4$ independent experiments). Data were analysed by two-way ANOVA followed by Bonferroni *post hoc* analysis.

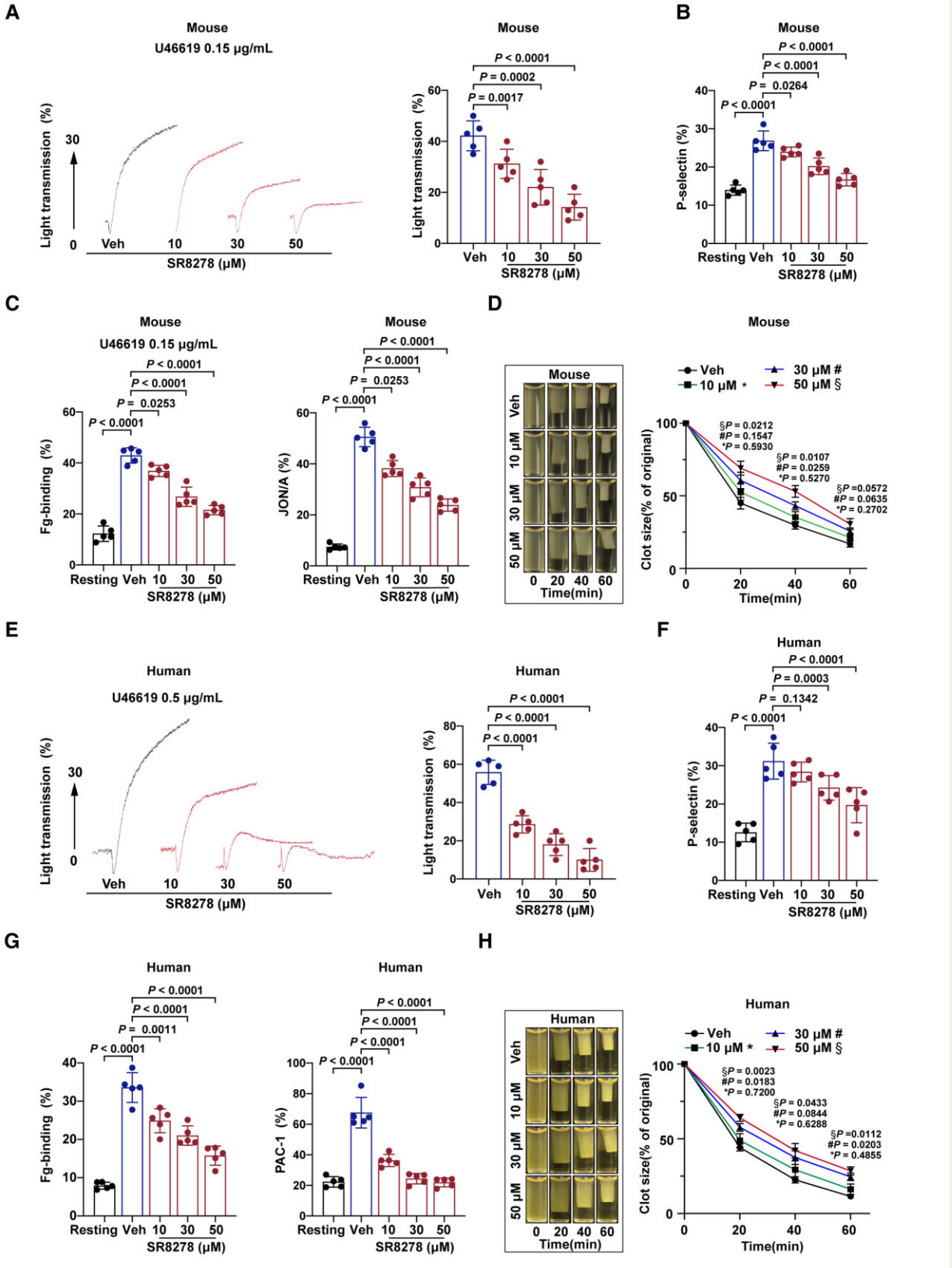

Figure 7 Pharmacological inhibition of Rev-erbα decreased multiple aspects of mouse and human platelet activation. Washed mouse and human platelets (2.5×10^8/ml) were pre-treated with vehicle or various concentrations of SR8278 (10–50 μM) for 30 min. SR8278 was dissolved in dimethyl sulfoxide (DMSO). The vehicles were treated with the same concentrations of DMSO, which were 0.1% in platelet suspension.

Continued

potentiates platelet activation via an OPHN-1-mediated RhoA/ERM signalling pathway.

Discussion

In the present work, we identified a novel role of the circadian nuclear receptor Rev-erbα in platelets. The novel contributions included the following: we detected two isoforms of Rev-erb (Rev-erbα and Rev-erbβ) in platelets from both humans and mice; however, only Rev-erbα showed a circadian rhythm that positively correlated with platelet aggregation. Global and platelet-specific knockout of Rev-erbα in mice decreased platelet activation and inhibited thrombus formation in multiple thrombosis models. Consistently, pharmacological inhibition of Rev-erbα by specific antagonists decreased human and mouse platelet aggregation and activation. Mechanistically, mass spectrometry and co-immunoprecipitation analyses revealed that Rev-erbα potentiated platelet activation via an OPHN-1-mediated RhoA/ERM signalling pathway (Structured Graphical abstract). Collectively, the current study provides the first evidence that Rev-erbα is expressed by platelets, positively regulates platelet activation, and contributes to thrombus formation through a non-genomic OPHN-1/RhoA/ERM signalling pathway.

Epidemiological studies revealed that adverse thrombotic events (i.e. acute myocardial infarction and ischaemic stroke) had day/night patterns, with peak onset in the early morning.[2,30] In accordance with the morning peak in adverse cardiovascular events, previous studies revealed that the highest platelet responses were shown in the morning hours, while the lowest were observed in the evening.[31–33] Moreover, surface markers expressed on the activated platelet, including activated αIIbβ3, P-selectin, and GPIb, reached a morning peak. The present study confirmed a circadian variation in platelet aggregation and thrombus propensity in human platelets, with a peak in the early morning at ∼9 a.m. However, the potential mechanism under the diurnal variation of platelets has not been appreciated.

Circadian rhythms are driven by the rhythmic oscillation of the endogenous circadian clock. In addition to the master circadian clock in the brain's hypothalamus, components of the circadian clock machinery are also expressed in various peripheral tissues and cells.[34] As a main peripheral circadian component, Rev-erbα belongs to the nuclear receptor superfamily (also known as nuclear receptor subfamily 1, group D, member 1; NR1D1).[14,16] Rev-erbα was initially considered to be an orphan nuclear receptor until 2007, when lipophilic haem was found as a physiologically relevant ligand of Rev-erbα.[35] Before long, a synthetic ligand for Rev-erbα (i.e. SR8278) was identified,[26] opening the door to novel pharmacological therapies based on Rev-erbα activity manipulation. Besides its classical functions on circadian rhythm, recent studies uncovered several new and unique functions and a broad involvement in the pathogenesis of various diseases.[11,36,37] Here, we reported our new findings that Rev-erbα was present in human and mouse platelets. Importantly, the expression of Rev-erbα showed a circadian rhythm that positively correlated with the platelet aggregation. Moreover, Rev-erbα was significantly upregulated in platelets from acute STEMI patients, with a peak at early morning. Collectively, these data identified circadian nuclear receptor Rev-erbα as a new functional protein expressed in platelets.

To determine whether platelet-expressed Rev-erbα mediates platelet activation or acts as an antiplatelet signal, we generated global and conditional Rev-erbα knockout mice. Although Rev-erbα deletion did not affect platelet counts, average platelet sizes and its microstructures, agonist-induced aggregation and multiple aspects of platelet activation were significantly impaired. Moreover, Rev-erbα depletion inhibited the ability of platelets to form thrombi in different *in vivo* thrombosis models, presented by prolonged mean time to carotid artery occlusion, less pulmonary vasculature thrombi formation, and resulted in significant protection against microvascular microthrombi obstruction and infarct expansion in a model of acute myocardial infarction. Of clinical relevance, we further examined the effects of pharmacological inhibition of Rev-erbα in human platelets. Consistent results of antiplatelet actions were obtained by Rev-erbα-specific antagonist SR8278 in human platelets. These lines

Figure 7 Continued

(*A*) Representative platelet aggregation tracings of SR8278-pre-treated mouse platelets stimulated with U46619, as indicated. Data are plotted in terms of percentage aggregation ($n = 5$ independent experiments). Data were analysed by one-way ANOVA test followed by Dunnett's multiple comparisons test. (*B*) Quantitation of P-selectin surface expression of mouse platelets stimulated with U46619, as indicated ($n = 5$ independent experiments). Data were analysed by two-way ANOVA test followed by Dunnett's multiple comparisons test. (*C*) Quantitation of flow cytometric analysis of Alexa Fluor 647-labelled fibrinogen-binding and PE-labelled JON/A-binding to SR8278-pre-treated washed mouse platelets stimulated with U46619, as indicated. Data are presented as a percentage of platelets binding to fibrinogen ($n = 5$ independent experiments). Data were analysed by two-way ANOVA test followed by Dunnett's multiple comparisons test. (*D*) Representative images of mouse platelet clot retraction stimulated with 0.5 U/ml thrombin. Images were captured every 20 for 60 min ($n = 4$ independent experiments). Data were analysed by two-way ANOVA test followed by Dunnett's multiple comparisons test. The two-dimensional size of the clot was measured using the ImageJ software. (*E*) Representative platelet aggregation tracings of SR8278-pre-treated human platelets stimulated with U46619, as indicated. Data are plotted in terms of percentage aggregation ($n = 5$ independent experiments). Data were analysed by one-way ANOVA test followed by Dunnett's multiple comparisons test. (*F*) Quantitation of P-selectin surface expression of human platelets stimulated with U46619, as indicated ($n = 5$ independent experiments). Data were analysed by two-way ANOVA test followed by Dunnett's multiple comparisons test. (*G*) Quantitation of flow cytometric analysis of Alexa Fluor 647-labelled fibrinogen-binding and fluoresceine isothiocyanate-labelled PAC-1-binding to SR8278-pre-treated washed human platelets stimulated with U46619, as indicated. Data are presented as a percentage of platelets binding to fibrinogen ($n = 5$ independent experiments). Data were analysed by two-way ANOVA test followed by Dunnett's multiple comparisons test. (*H*) Representative images of human platelet clot retraction stimulated with 0.2 U/ml thrombin. Images were captured every 20 min for 60 min. The data are plotted in terms of clot size. The two-dimensional size of the clot was measured using the ImageJ software ($n = 4$ independent experiments). Data were analysed by two-way ANOVA test followed by Dunnett's multiple comparisons test. **P* indicates the comparison between vehicle and 10 μM SR8278-treated platelets; $^{\#}P$, vehicle and 30 μM SR8278-treated; $^{\S}P$, vehicle; and 50 μM SR8278-treated. Veh indicates vehicle.

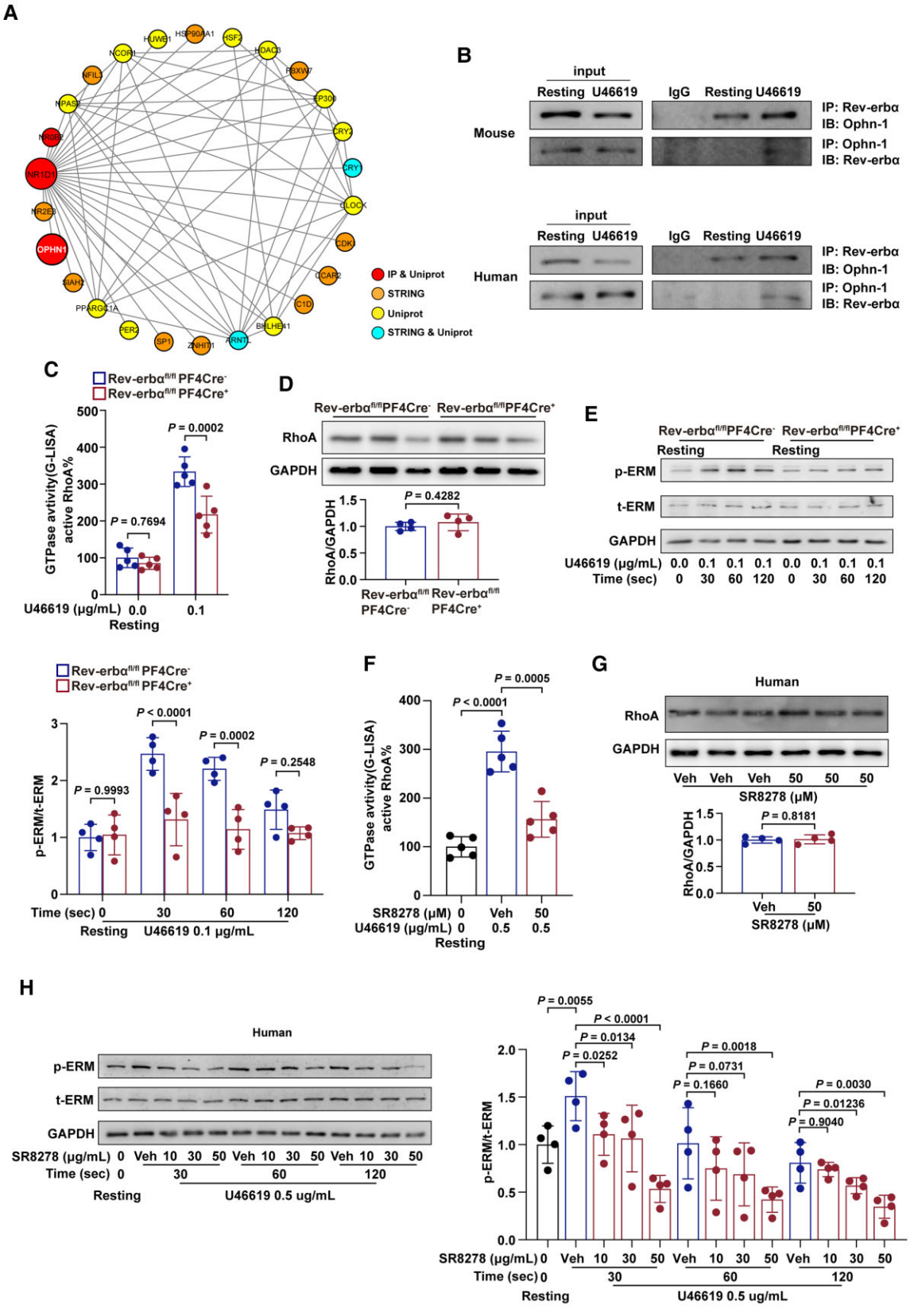

Figure 8 Rev-erbα interacted with OPHN-1, promoted RhoA activity and phosphorylation of ERM. (*A*) The protein–protein interaction analysis showed the top-ranked protein. (*B*) Rabbit anti-Rev-erbα monoclonal antibody was used to immunoprecipitate Rev-erbα from the lysates of resting

Continued

of evidence convincingly pointed out a previously unrecognized role of Rev-erbα as a positive regulator contributing to platelet activation and thrombus formation.

As a transcription factor, Rev-erbα has been well characterized to function by transcriptionally regulating downstream gene targets in nucleated cells.[38] Binding via the DBD to the ROR response element DNA sequence (RORE), Rev-erbα would recruit nuclear receptor corepressor to play a critical role in transcriptional control in various nucleated cells. However, platelets are anucleate cells, and thus, it is quite interesting to investigate how circadian nuclear receptor Rev-erbα regulates anucleate platelet functions. Based on the results of mass spectrometry and the protein–protein interaction network analysis, OPHN-1 was identified as a candidate protein for Rev-erbα actions in platelets. Co-immunoprecipitation analyses confirmed that Rev-erbα interacted with OPHN-1 in both mouse and human platelets, and this interaction significantly increased upon stimulation with agonists. Oligophrenin-1 is a RhoGAP-regulating cytoplasmic protein that exhibits strong GTPase-stimulating activity towards the Rho-family small GTPases RhoA.[29] As a main downstream target of OPHN-1, RhoA regulates actin cytoskeleton and promotes actin remodelling in platelets,[38] which is crucial for platelet activation. RhoA deletion decreased platelet aggregation and multiple aspects of platelet activation,[39] while OPHN-1 deletion promoted thrombus formation through aberrant Rho activation.[40] Here, genetic deletion or pharmacological inhibition of Rev-erbα significantly downregulated the activity of RhoA without altering RhoA expression in platelets. Moreover, the phosphorylation levels of ERM proteins, a downstream effector of RhoA, were significantly downregulated. ERM signalling is regulated by Rho via phosphorylation at Thr558 of the moesin phosphatase, and implicated in the formation of filopodia and lamellipodia in platelets.[41,42] All together, these results revealed that Rev-erbα potentiated platelet activation, at least partially, via an OPHN-1/RhoA/ERM signalling pathway.

The involvement of Rev-erbα in regulating cell functions has also been reported in other cell types.[11,43–45] Rev-erbα was shown to be a positive regulator that contributed to the amyloid plaque deposition in Alzheimer's disease by targeting microglial cells.[46] However, it functioned as a negative regulator in pulmonary inflammation[43] and neuroinflammation.[44] Thus, the role of Rev-erbα in regulating cell functions may depend on the cell types, and platelet-targeted Rev-erbα inhibition would be an optimal choice for clinical implications.[45]

Clinical implications of this study

The current experimental findings are scientifically and clinically important. The identification of circadian nuclear receptor Rev-erbα as a novel functional protein in platelets may broaden our understanding of the multiple biological functions of Rev-erbα. Our observations, along with the recent findings regarding the diurnal oscillation of platelet aggregation,[6,47,48] highlight the importance of circadian clock machinery in platelet physiology. Importantly, the finding of the ability of regulating platelet aggregation and thrombus formation, which often precipitates stroke or myocardial infarction, supports that Rev-erbα may serve as a novel therapeutic target for managing thrombosis-based cardiovascular diseases.

Supplementary material

Supplementary material is available at *European Heart Journal* online.

Acknowledgments

We are greatly appreciative of Prof. Junling Liu in the Department of Biochemistry and Molecular Cell Biology, Key Laboratory of Cell Differentiation, and Apoptosis of Chinese Ministry of Education, School of Medicine, Shanghai Jiao Tong University, for his expertise in platelet biology and activation.

Figure 8 Continued

Rev-erbα$^{fl/fl}$Cre^{-} platelets and U46619-stimulated Rev-erbα$^{fl/fl}$Cre^{-} platelets. Rabbit IgG was used as the negative control. Mouse anti-OPHN-1 monoclonal antibody was used to immunoprecipitate OPHN-1 from the lysates of resting Rev-erbα$^{fl/fl}$Cre^{-} platelets and U46619-stimulated Rev-erbα$^{fl/fl}$Cre^{-} platelets. Mouse IgG was used as negative controls. The human platelets were subjected to co-immunoprecipitation assay using the same method ($n = 4$ independent experiments). (*C*) Active GTP-bound RhoA in Rev-erbα$^{fl/fl}$Cre^{-} and Rev-erbα$^{fl/fl}$PF4Cre^{+} platelets stimulated with U46619 (0.1 μg/ml) were analysed using G-LISA ($n = 5$ independent experiments). Data were analysed by two-way ANOVA test followed by Bonferroni *post hoc* analysis. (*D*) RhoA protein expression in the Rev-erbα$^{fl/fl}$Cre^{-} and Rev-erbα$^{fl/fl}$PF4Cre^{+} platelets. Quantification of the ratio of RhoA to GAPDH ($n = 4$ independent experiments). Data were analysed by Student's *t*-test. (*E*) Detection of phosphorylated ezrin (Thr567)/radixin (Thr564)/moesin (Thr558)(p-ERM) in Rev-erbα$^{fl/fl}$Cre^{-} and Rev-erbα$^{fl/fl}$PF4Cre^{+} platelets using phospho-specific antibodies. Total amounts of ezrin/radixin/moesin(t-ERM) and GAPDH (loading control) in platelet lysates. Quantification of the ratio of p-ERM to t-ERM ($n = 4$ independent experiments). Data were analysed by two-way ANOVA test followed by Bonferroni *post hoc* analysis. (*F*) SR8278 was dissolved in DMSO. The vehicles were treated with the same concentrations of DMSO, which were 0.1% in platelet suspension. Active GTP-bound RhoA in untreated resting, U46619 (0.5 μg/ml)-treated, and SR8278 (50 μM) + U46619 (0.5 μg/ml)-treated human platelets were analysed using G-LISA ($n = 5$ independent experiments). Data were analysed by two-way ANOVA test followed by Dunnett's multiple comparisons test. (*G*) RhoA protein expression in the vehicle controls and SR8278 (50 μM)-treated human platelets. Quantification of the ratio of RhoA to GAPDH ($n = 4$ independent experiments). Data were analysed by Student's *t*-test. (*H*) Detection of phosphorylated ERM in untreated resting, U46619 (0.5 μg/ml)-treated, SR8278 (10 μM) + U46619 (0.5 μg/ml)-treated, SR8278 (30 μM) + U46619 (0.5 μg/ml)-treated, and SR8278 (50 μM) + U46619 (0.5 μg/ml)-treated human platelets using phospho-specific antibodies. Total amounts of ERM and GAPDH (loading control) in platelet lysates. Quantification of the ratio of p-ERM to t-ERM ($n = 4$ independent experiments). Data were analysed by two-way ANOVA test followed by Dunnett's multiple comparisons test. Veh indicates vehicle.

Funding

This work was supported by grants from the National Science Fund for Distinguished Young Scholars (81625002), the National Natural Science Foundation of China (81930007, 91839301, 81470389, 81800307, 81500221), the Shanghai Outstanding Academic Leaders Program (18XD1402400), Shanghai Municipal Key Clinical Specialty (shslczdzk06204), and the Science and Technology Commission of Shanghai Municipality (201409005200).

Conflict of interest: none declared.

Author contributions

J.P. conceived the study; J.S., R.T., M.Z., and Y.G. performed the experiments; J.S., R.T., M.Z., Y.G., and W.L. analysed the data; Y.Z., Y.C., D.L., G.M., G.L., A.Y., and L.H. prepared the figures; J.S., R.T., and M.Z. drafted the manuscript; J.P. reviewed the manuscript.

References

1. van der Meijden PEJ, Heemskerk JWM. Platelet biology and functions: new concepts and clinical perspectives. *Nat Rev Cardiol* 2019;**16**:166–179.
2. Thosar SS, Butler MP, Shea SA. Role of the circadian system in cardiovascular disease. *J Clin Invest* 2018;**128**:2157–2167.
3. Crnko S, Du Pré BC, Sluijter JPG, Van Laake LW. Circadian rhythms and the molecular clock in cardiovascular biology and disease. *Nat Rev Cardiol* 2019;**16**:437–447.
4. Tofler GH, Brezinski D, Schafer AI, Czeisler CA, Rutherford JD, Willich SN, *et al.* Concurrent morning increase in platelet aggregability and the risk of myocardial infarction and sudden cardiac death. *N Engl J Med* 1987;**316**:1514–1518.
5. Scheer FAJL, Michelson AD, Frelinger AL, Evoniuk H, Kelly EE, McCarthy M, *et al.* The human endogenous circadian system causes greatest platelet activation during the biological morning independent of behaviors. *PLoS One* 2011;**6**:e24549.
6. Jafri SM, VanRollins M, Ozawa T, Mammen EF, Goldberg AD, Goldstein S. Circadian variation in platelet function in healthy volunteers. *Am J Cardiol* 1992;**69**:951–954.
7. Burris TP. Nuclear hormone receptors for heme: REV-ERBalpha and REV-ERBbeta are ligand-regulated components of the mammalian clock. *Mol Endocrinol* 2008;**22**:1509–1520.
8. Sulli G, Rommel A, Wang X, Kolar MJ, Puca F, Saghatelian A, *et al.* Pharmacological activation of REV-ERBs is lethal in cancer and oncogene-induced senescence. *Nature* 2018;**553**:351–355.
9. Yu D, Fang X, Xu Y, Xiao H, Huang T, Zhang Y, *et al.* Rev-erbα can regulate the NF-κB/NALP3 pathway to modulate lipopolysaccharide-induced acute lung injury and inflammation. *Int Immunopharmacol* 2019;**73**:312–320.
10. Solt LA, Wang Y, Banerjee S, Hughes T, Kojetin DJ, Lundasen T, *et al.* Regulation of circadian behaviour and metabolism by synthetic REV-ERB agonists. *Nature* 2012;**485**:62–68.
11. Montaigne D, Marechal X, Modine T, Coisne A, Mouton S, Fayad G, *et al.* Daytime variation of perioperative myocardial injury in cardiac surgery and its prevention by Rev-Erbα antagonism: a single-centre propensity-matched cohort study and a randomised study. *Lancet* 2018;**391**:59–69.
12. Wang N, Sun Y, Zhang H, Wang B, Chen C, Wang Y, *et al.* Long-term night shift work is associated with the risk of atrial fibrillation and coronary heart disease. *Eur Heart J* 2021;**42**:4180–4188.
13. Pu J, Ding S, Ge H, Han Y, Guo J, Lin R, *et al.* Efficacy and safety of a pharmaco-invasive strategy with half-dose alteplase versus primary angioplasty in ST-segment–elevation myocardial infarction: EARLY-MYO trial (Early routine catheterization after alteplase fibrinolysis versus primary PCI in acute ST-segment–elevation myocardial infarction). *Circulation* 2017;**136**:1462–1473.
14. Preitner N, Damiola F, Lopez-Molina L, Zakany J, Duboule D, Albrecht U, *et al.* The orphan nuclear receptor REV-ERBalpha controls circadian transcription within the positive limb of the mammalian circadian oscillator. *Cell* 2002;**110**:251–260.
15. Lazar MA, Hodin RA, Darling DS, Chin WW. A novel member of the thyroid/steroid hormone receptor family is encoded by the opposite strand of the rat c-erbA alpha transcriptional unit. *Mol Cell Biol* 1989;**9**:1128–1136.
16. Duez H, Staels B. Rev-erb-alpha: an integrator of circadian rhythms and metabolism. *J Appl Physiol (1985)* 2009;**107**:1972–1980.
17. Muller JE, Stone PH, Turi ZG, Rutherford JD, Czeisler CA, Parker C, *et al.* Circadian variation in the frequency of onset of acute myocardial infarction. *N Engl J Med* 1985;**313**:1315–1322.
18. Nakanishi H, Ni J, Nonaka S, Hayashi Y. Microglial circadian clock regulation of microglial structural complexity, dendritic spine density and inflammatory response. *Neurochem Int* 2021;**142**:104905.
19. Deutsch VR, Tomer A. Megakaryocyte development and platelet production. *Br J Haematol* 2006;**134**:453–466.
20. Forrester KR, Tulip J, Leonard C, Stewart C, Bray RC. A laser speckle imaging technique for measuring tissue perfusion. *IEEE Trans Biomed Eng* 2004;**51**:2074–2084.
21. Hastings SM, Griffin MT, Ku DN. Hemodynamic studies of platelet thrombosis using microfluidics. *Platelets* 2017;**28**:427–433.
22. Qi Z, Hu L, Zhang J, Yang W, Liu X, Jia D, *et al.* PCSK9 (Proprotein Convertase Subtilisin/Kexin 9) enhances platelet activation, thrombosis, and myocardial infarct expansion by binding to platelet CD36. *Circulation* 2021;**143**:45–61.
23. Polgar J, Matuskova J, Wagner DD. The P-selectin, tissue factor, coagulation triad. *J Thromb Haemost* 2005;**3**:1590–1596.
24. Huang J, Li X, Shi X, Zhu M, Wang J, Huang S, *et al.* Platelet integrin αIIbβ3: signal transduction, regulation, and its therapeutic targeting. *J Hematol Oncol* 2019;**12**:26.
25. Flevaris P, Stojanovic A, Gong H, Chishti A, Welch E, Du X. A molecular switch that controls cell spreading and retraction. *J Cell Biol* 2007;**179**:553–565.
26. Kojetin D, Wang Y, Kamenecka TM, Burris TP. Identification of SR8278, a synthetic antagonist of the nuclear heme receptor REV-ERB. *ACS Chem Biol* 2011;**6**:131–134.
27. Zhang T, Zhao M, Lu D, Wang S, Yu F, Guo L, *et al.* REV-ERB *α* regulates CYP7A1 through repression of liver receptor homolog-1. *Drug Metab Dispos* 2018;**46**:248–258.
28. Trump RP, Bresciani S, Cooper AWJ, Tellam JP, Wojno J, Blaikley J, *et al.* Optimized chemical probes for REV-ERBα. *J Med Chem* 2013;**56**:4729–4737.
29. Aslan JE. Platelet Rho GTPase regulation in physiology and disease. *Platelets* 2019;**30**:17–22.
30. Morning peak in the incidence of myocardial infarction: experience in the ISIS-2 trial. ISIS-2 (Second International Study of Infarct Survival) Collaborative Group. *Eur Heart J* 1992;**13**:594–598.
31. Budkowska M, Lebiecka A, Marcinowska Z, Woźniak J, Jastrzębska M, Dołęgowska B. The circadian rhythm of selected parameters of the hemostasis system in healthy people. *Thromb Res* 2019;**182**:79–88.
32. Paschos GK, FitzGerald GA. Circadian clocks and vascular function. *Circ Res* 2010;**106**:833–841.
33. Curtis AM, Fitzgerald GA. Central and peripheral clocks in cardiovascular and metabolic function. *Ann Med* 2006;**38**:552–559.
34. Reppert SM, Weaver DR. Molecular analysis of mammalian circadian rhythms. *Annu Rev Physiol* 2001;**63**:647–676.
35. Kojetin DJ, Burris TP. REV-ERB and ROR nuclear receptors as drug targets. *Nat Rev Drug Discov* 2014;**13**:197–216.
36. Pourcet B, Zecchin M, Ferri L, Beauchamp J, Sitaula S, Billon C, *et al.* Nuclear receptor subfamily 1 Group D member 1 regulates circadian activity of NLRP3 inflammasome to reduce the severity of fulminant hepatitis in mice. *Gastroenterology* 2018;**154**:1449–1464.e20.
37. Zhang T, Yu F, Xu H, Chen M, Chen X, Guo L, *et al.* Dysregulation of REV-ERBα impairs GABAergic function and promotes epileptic seizures in preclinical models. *Nat Commun* 2021;**12**:1216.
38. Wang S, Li F, Lin Y, Wu B. Targeting REV-ERBα for therapeutic purposes: promises and challenges. *Theranostics* 2020;**10**:4168–4182.
39. Pleines I, Hagedorn I, Gupta S, May F, Chakarova L, van Hengel J, *et al.* Megakaryocyte-specific RhoA deficiency causes macrothrombocytopenia and defective platelet activation in hemostasis and thrombosis. *Blood* 2012;**119**:1054–1063.
40. Fotinos A, Klier M, Gowert NS, Münzer P, Klatt C, Beck S, *et al.* Loss of oligophrenin1 leads to uncontrolled Rho activation and increased thrombus formation in mice. *J Thromb Haemost* 2015;**13**:619–630.
41. Jeon S, Kim S, Park J-B, Suh P-G, Kim YS, Bae C-D, *et al.* RhoA and Rho kinase-dependent phosphorylation of moesin at Thr-558 in hippocampal neuronal cells by glutamate. *J Biol Chem* 2002;**277**:16576–16584.
42. Nakamura F, Huang L, Pestonjamasp K, Luna EJ, Furthmayr H. Regulation of F-Actin binding to platelet moesin in vitro by both phosphorylation of threonine 558 and polyphosphatidylinositides. *Mol Biol Cell* 1999;**10**:2669–2685.
43. Wang Q, Sundar IK, Lucas JH, Muthumalage T, Rahman I. Molecular clock REV-ERBα regulates cigarette smoke-induced pulmonary inflammation and epithelial-mesenchymal transition. *JCI Insight* 2021;**6**:145200.
44. Kim J, Jang S, Choi M, Chung S, Choe Y, Choe HK, *et al.* Abrogation of the circadian nuclear receptor REV-ERBα exacerbates 6-hydroxydopamine-induced dopaminergic neurodegeneration. *Mol Cells* 2018;**41**:742–752.
45. Wang F, Li X, Zhou Y, Zhang Y, Chen X, Yang J, *et al.* Nanoscaled polyion complex micelles for targeted delivery of recombinant hirudin to platelets based on cationic copolymer. *Mol Pharm* 2010;**7**:718–726.
46. Lee J, Kim DE, Griffin P, Sheehan PW, Kim D-H, Musiek ES, *et al.* Inhibition of REV-ERBs stimulates microglial amyloid-beta clearance and reduces amyloid plaque deposition in the 5XFAD mouse model of Alzheimer's disease. *Aging Cell* 2020;**19**:e13078.
47. Diurnal variation in platelet aggregation responses. *Lancet* 1988;**332**:1405–1406.
48. Ohkura N, Oishi K, Sudo T, Hayashi H, Shikata K, Ishida N, *et al.* CLOCK regulates circadian platelet activity. *Thromb Res* 2009;**123**:523–527.